Statistical analysis of photonuclear interactions of muons in iron

First-year doctoral qualifying exams- Statistical Treatment and Analysis of the Data

Martina Cucinotta





Introduction

General information:

- Introduction to the analysis
- Experimental setup
- Analysed data
- Observables and event selection

Statistical treatment:

- Nuisance parameters & post fit distribution
- Confidence interval estimate
- Assessment of the asymptotic behavior

Conclusions

Eur. Phys. J. C 28, 297–304 (2003)
Digital Object Identifier (DOI) 10.1140/epjc/s2003-01176-6

THE EUROPEAN PHYSICAL JOURNAL C

https://link.springer.com/article/10.1140/epic/s2003-01176-6

 The goal of this analysis is the study of muon photonuclear reactions in iron using data from the TileCal test beam

$$\mu + A \rightarrow \mu^I + hadrons + X (\sigma_{TH}^{\sim} 24 \mu b)$$

High-energy muons → Account for hadronic showers along muon tracks in energy flow (hadron background).

MIP response measurement → Set absolute energy scale for cell calibration.

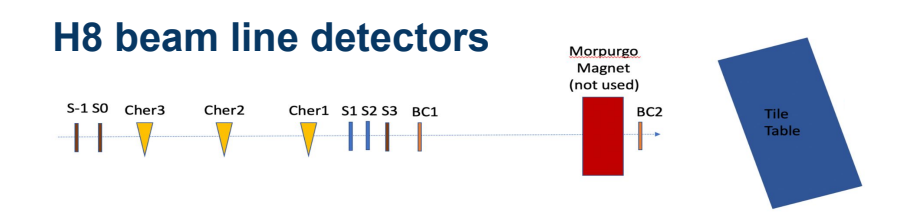
A measurement of the photonuclear interactions of 180 GeV muons in iron

The TileCal System of the ATLAS Collaboration

```
C. Alexa<sup>6</sup>, K. Anderson<sup>7</sup>, A. Antonaki<sup>3</sup>, V. Batusov<sup>9</sup>, S. Berglund<sup>20</sup>, C. Biscarat<sup>8</sup>, O. Blanch<sup>4</sup>, G. Blanchot<sup>4</sup>
 A. Bogush<sup>13</sup>, C. Bohm<sup>20</sup>, V. Boldea<sup>6</sup>, M. Bosman<sup>4</sup>, C. Bromberg<sup>10</sup>, J. Budagov<sup>9</sup>, L. Caloba<sup>19</sup>, D. Calvet<sup>8</sup>
F. Camarena<sup>23</sup>, J. Carvalho<sup>12b</sup>, J. Castelo<sup>23</sup>, M. V. Castillo<sup>23</sup>, M. Cavalli-Sforza<sup>4</sup>, V. Cavasinni<sup>15</sup>, A. S. Cerqueira<sup>19</sup>
 M. Cobal<sup>11</sup>, F. Cogswell<sup>22</sup>, S. Constantinescu<sup>6</sup>, D. Costanzo<sup>15</sup>, B. Cowan<sup>7</sup>, C. Cuenca<sup>23</sup>, D. O. Damazio<sup>19</sup>
 M. David<sup>12a</sup>, T. Davidek<sup>16</sup>, K. De<sup>2</sup>, M. Delfino<sup>4</sup>, T. Del Prete<sup>15</sup>, B. Di Girolamo<sup>11</sup>, S. Dita<sup>6</sup>, J. Dolejsi<sup>16</sup>
Z. Dolezal<sup>16</sup>, A. Dotti<sup>15</sup>, R. Downing<sup>22</sup>, I. Efthymiopoulos<sup>11</sup>, M. Engström<sup>20</sup>, D. Errede<sup>22</sup>, S. Errede<sup>22</sup>, F. Fassi<sup>23</sup>
D. Fassouliotis<sup>3</sup>, I. Fedorko<sup>5</sup>, A. Fenyuk<sup>18</sup>, C. Ferdi<sup>8</sup>, A. Ferrer<sup>23</sup>, V. Flaminio<sup>15</sup>, J. Flix<sup>4</sup>, E. Fullana<sup>23</sup>, R. Garabik<sup>5</sup>
V. Garde<sup>8</sup>, V. Giakoumopoulou<sup>3</sup>, O. Gildemeister<sup>11</sup>, V. Gilewsky<sup>13</sup>, N. Giokaris<sup>3</sup>, A. Gomes<sup>12a</sup>, V. Gonzalez<sup>23</sup>
S. González De La Hoz<sup>23</sup>, V. Grabsky<sup>24</sup>, P. Grenier<sup>11</sup>, P. Gris<sup>8</sup>, V. Guarino<sup>1</sup>, C. Guicheney<sup>8</sup>, A. Gupta<sup>7</sup>
H. Hakobyan<sup>24</sup>, M. Haney<sup>22</sup>, A. Henriques<sup>11</sup>, E. Higon<sup>23</sup>, S. Holmgren<sup>20</sup>, J. Huston<sup>10</sup>, C. Iglesias<sup>4</sup>, K. Jon-And<sup>20</sup>, T. Junk<sup>22</sup>, A. Karyukhin<sup>18</sup>, J. Khubua<sup>9,21</sup>, S. Kopikov<sup>18</sup>, I. Korolkov<sup>4</sup>, P. Krivkova<sup>16</sup>, Y. Kulchitsky<sup>13,9</sup>, P. Kuzhir<sup>14</sup>
 V. Lapin<sup>18</sup>, T. Le Compte<sup>1</sup>, R. Lefevre<sup>8</sup>, R. Leitner<sup>16</sup>, M. Lembesi<sup>3</sup>, J. Li<sup>2</sup>, M. Liablin<sup>9</sup>, Y. Lomakin<sup>9</sup>, M. Lokajicek<sup>17</sup>
J. M. Lopez Amengual<sup>23</sup>, A. Maio<sup>12a</sup>, S. Maliukov<sup>9</sup>, A. Manousakis<sup>3</sup>, C. Marques<sup>12a</sup>, F. Marroquim<sup>19</sup>, F. Martin<sup>8</sup>
 E. Mazzoni<sup>15</sup>, F. Merritt<sup>7</sup>, R. Miller<sup>10</sup>, I. Minashvili<sup>9</sup>, L. Miralles<sup>4</sup>, G. Montarou<sup>8</sup>, S. Nemecek<sup>17</sup>, M. Nessi<sup>11</sup>
 L. Nodulman<sup>1</sup>, O. Norniella<sup>4</sup>, A. Onofre<sup>12c</sup>, M. Oreglia<sup>7</sup>, A. Pacheco<sup>4</sup>, D. Pallin<sup>8</sup>, D. Pantea<sup>6</sup>, J. Pilcher<sup>7</sup>, J. Pina<sup>12a</sup>
J. Pinh˜ao<sup>12b</sup>, F. Podlyski<sup>8</sup>, X. Portell<sup>4</sup>, L. E. Price<sup>1</sup>, J. Proudfoot<sup>1</sup>, R. Richards<sup>10</sup>, C. Roda<sup>15</sup>, V. Romanov<sup>9</sup>
 P. Rosnet<sup>8</sup>, P. Roy<sup>8</sup>, V. Rumiantsau<sup>14</sup>, N. Russakovich<sup>9</sup>, B. Salvachua<sup>23</sup>, E. Sanchis<sup>23</sup>, H. Sanders<sup>7</sup>, C. Santoni<sup>8</sup>
J. G. Saraiva<sup>12a</sup>, I. Satsunkevitch<sup>13</sup>, L.-P. Says<sup>8</sup>, J. Schlereth<sup>1</sup>, J. M. Seixas<sup>19</sup>, B. Selldèn<sup>20</sup>, N. Shalanda<sup>18</sup>.
 P. Shevtsov<sup>14</sup>, M. Shochet<sup>7</sup>, J. Silva<sup>12a</sup>, V. Simaitis<sup>22</sup>, A. Sissakian<sup>9</sup>, J. Sjölin<sup>20</sup>, S. Soares<sup>12a</sup>, A. Solodkov<sup>18</sup>
O. Solovianov<sup>18</sup>, M. Sosebee<sup>2</sup>, R. Stanek<sup>1</sup>, E. Starchenko<sup>18</sup>, P. Starovoitov<sup>14</sup>, P. Stavina<sup>5</sup>, M. Suk<sup>16</sup>, I. Sykora<sup>5</sup>,
 F. Tang<sup>7</sup>, P. Tas<sup>16</sup>, R. Teuscher<sup>7</sup>, S. Tokar<sup>5</sup>, N. Topilin<sup>9</sup>, J. Torres<sup>23</sup>, V. Tsulaia<sup>9</sup>, D. Underwood<sup>1</sup>, G. Usai<sup>15</sup>
S. Valkar<sup>16</sup>, M. J. Varanda<sup>12a</sup>, A. Vartapetian<sup>2</sup>, F. Vazeille<sup>8</sup>, I. Vichou<sup>3</sup>, V. Vinogradov<sup>9</sup>, I. Vivarelli<sup>15</sup>, A. White<sup>2</sup>,
 A. Zaitsev<sup>18</sup>, T. Zenis<sup>5</sup>
```

This presentation represents an initial statistical approach to revisiting that analysis.

TileCal test beam experimental setup



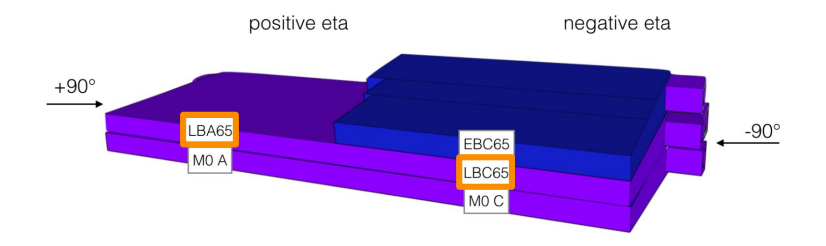
 TileCal test beam are performed in the H8 line from SPS in the CERN North Area.

TileCal test beam experimental setup

H8 beam line detectors S-150 Cher3 Cher2 Cher1 S1 S2 S3 BC1 BC2 Tile Table

 TileCal test beam are performed in the H8 line from SPS in the CERN North Area.

 Three overlapping TileCal modules (2 long barrels and 1 extended barrel)



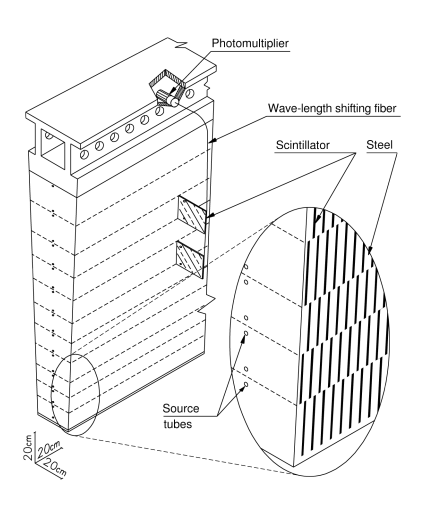
TileCal test beam experimental setup

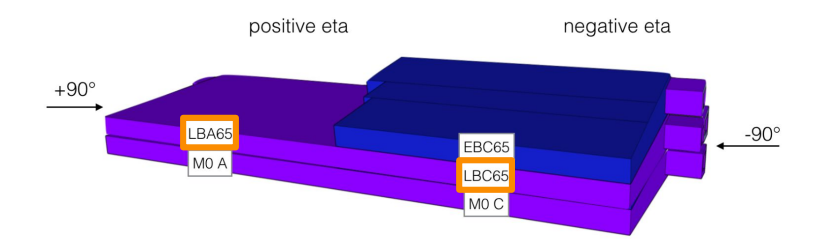
H8 beam line detectors



 TileCal test beam are performed in the H8 line from SPS in the CERN North Area.

 Three overlapping TileCal modules (2 long barrels and 1 extended barrel).



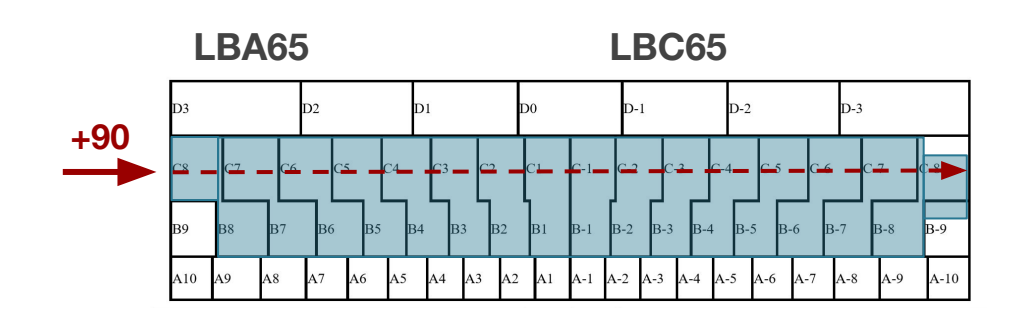


 Sampling calorimeter → each module is made of alternating scintillator and iron tiles. The long and extended barrel modules differ in geometry and number of cells.

Analysed run

The run under analysis was acquired during the September 2024 test beam campaign.

- Energy: 160 GeV
- High statistic run: 1981949 events
- Longitudinal muons: incidence angle +90°



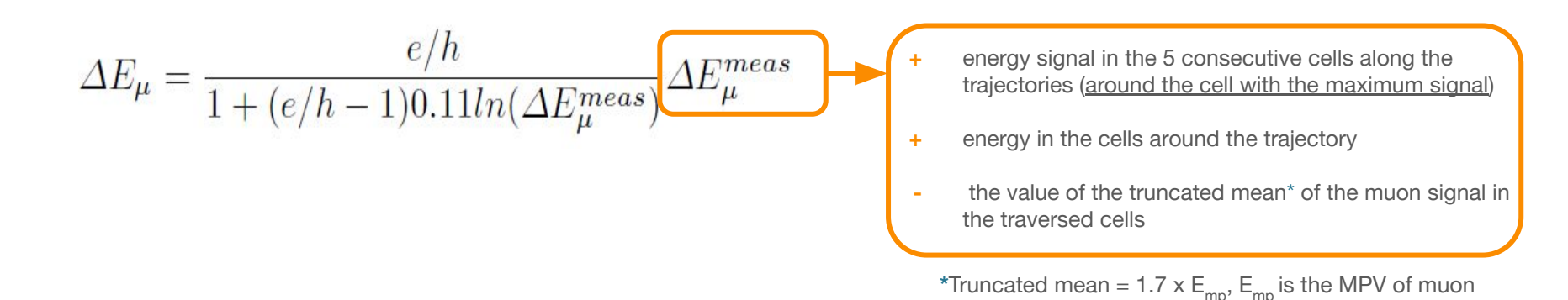
• What are we looking for?

Muon events with an energy deposit, off the trajectory, compatible with that of a hadronic shower.

$$\mu\text{+}A \rightarrow \mu^I + hadrons + X$$

Muon energy loss

• Part of the muon energy loss (ΔE_{μ}^{meas}) generates the hadronic shower. This energy loss has been calculated and corrected according to the following relation:



energy for each cell.

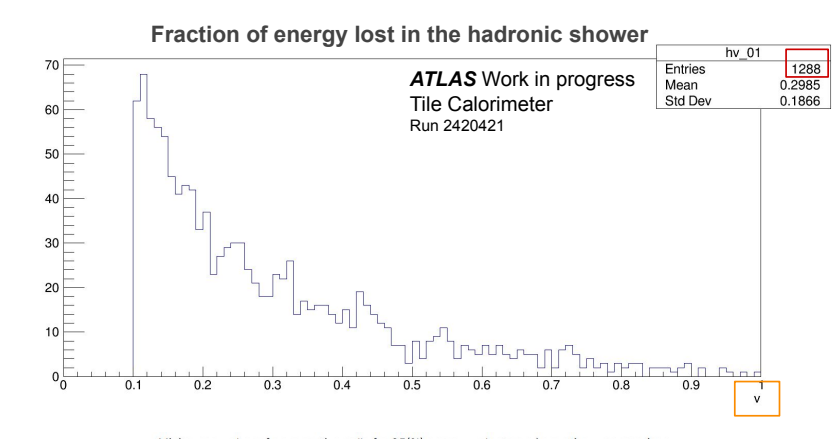
◆ The normalization factor is due to the "non-compensative" behaviour of TileCal (e/h = 1.35 ± 0.05)

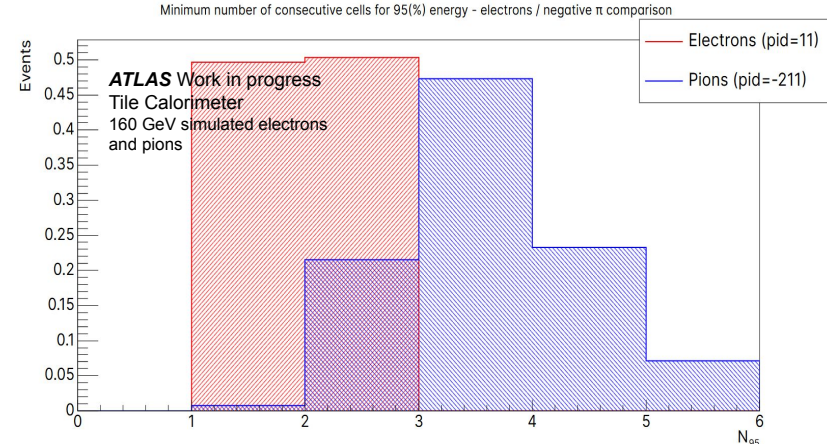
Observables

 The observables used to discriminate signal and background are the muon fractional energy loss (v) and N₉₅:

$$v = \Delta E_{\mu}/(E_{\mu} - \epsilon)$$

N₉₅ is defined as the minimum number of cells, within a window of 5 longitudinal consecutive cells, in which 95% of the total energy deposited by the shower is contained.





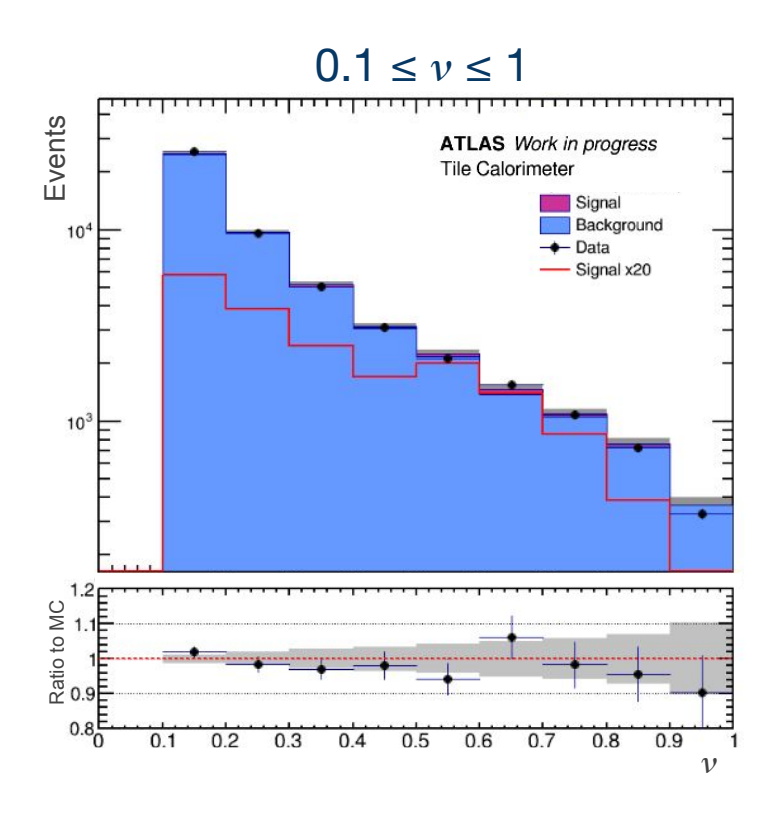
Data and MC sample

- Data were acquired by exposing the test beam setup to a low-intensity muon beam with an energy of 160 GeV. A total of 1,981,949 events were collected during this run.
- Muons with an energy of 160 GeV interacting with the test beam setup were generated in Monte Carlo (MC) simulations. The simulation was carried out using the Athena framework, with an accurate implementation of the TileCal test beam geometry. The number of simulated muons is 500,000.
- ◆ The total number of generated MC events corresponds to approximately one quarter of the events in the dataset. For this reason, a scale factor K has been included in the statistical treatment of the MC events.

Event selection and categorization

- The analysis is based on the availability of both a signal template and a background template, which model the expected distributions of the respective components.
- Signal region defined requiring:
 - At least one cell outside the track with an energy deposit of at least 0.75 GeV (typical of a hadronic shower)
 - $N_{op} \ge 3$ to reject the knock-on electrons or radiative losses from muons
 - Required v > 0.1 to suppress electron background.
- An estimate of the background was derived from a dedicated control region and propagated to the signal region using a scale factor. As a simplifying assumption, the scale factor was fixed to 1 (additional details available in the backup slides).

Pre-fit distributions for ν



 Low energy fractions deposited off-trajectory are dominated by background events (knock-on electron showers, bremsstrahlung and pair production), therefore the 0 ≤ v ≤ 0.1 region is excluded from the analysis.

The distribution is background-dominated

Statistical method

The goal of the analysis is to estimate the **signal strength** (μ) of the process under study using a <u>likelihood fit</u>. The signal strength is defined as:

$$\mu = rac{\sigma_{
m meas}}{\sigma_{
m MC}}$$
 $\sigma_{
m meas}^{
m meas}$ is the

 $\mu = rac{\sigma_{
m meas}}{\sigma_{
m MC}}$ $\sigma_{
m meas}$ is the measured cross section $\sigma_{
m MC}$ is the cross section predicted by MC simulations

The likelihood model has been constructed using the y > 0.1 distribution. Assuming the bins are independent, and introducing a global scale factor K, the total probability of observing all the counts is:

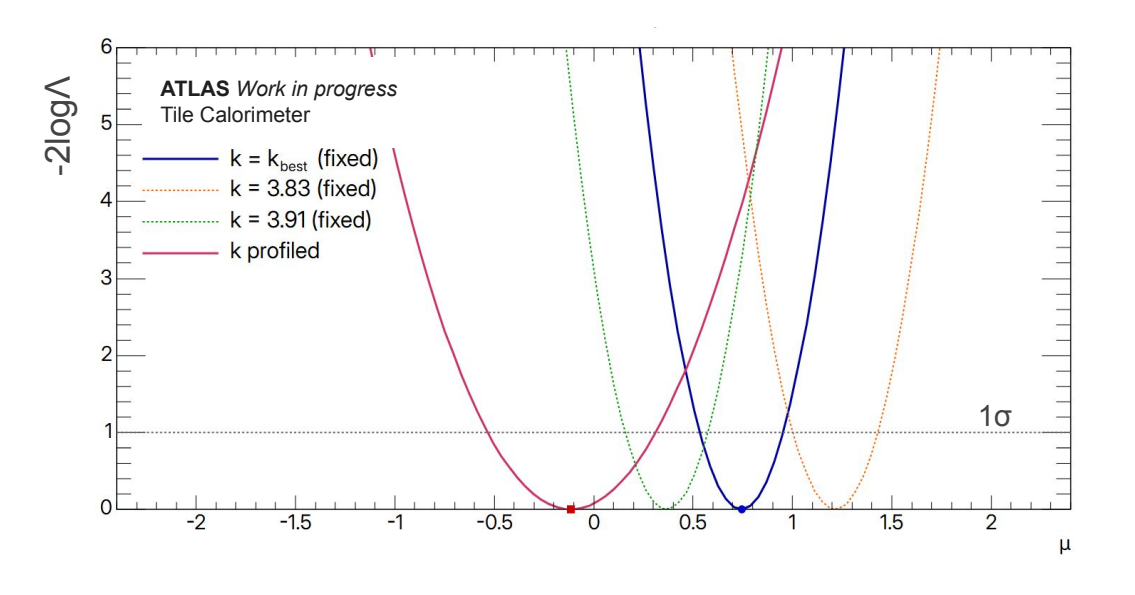
$$\mathcal{L}(\mu,k) = \prod_{i} \operatorname{Pois}(n_i \mid k(\mu s_i + b_i)) \quad \text{where:} \quad \text{n}_i \text{ is the observed number of events in bin i,} \\ \text{s}_i \text{ and b}_i \text{ are the expected signal and background yields in bin i,} \\ \text{μ is the signal strength,} \\ \text{k is a scale factor for both signal and background predictions.}$$

For simplicity, the analysis is performed using the negative log-likelihood, specifically -2logL, which allows for easier numerical minimization and statistical interpretation.

$$-2\log\mathcal{L} = 2\sum_i \left[k(\mu s_i + b_i) - n_i\log(k(\mu s_i + b_i))
ight]$$

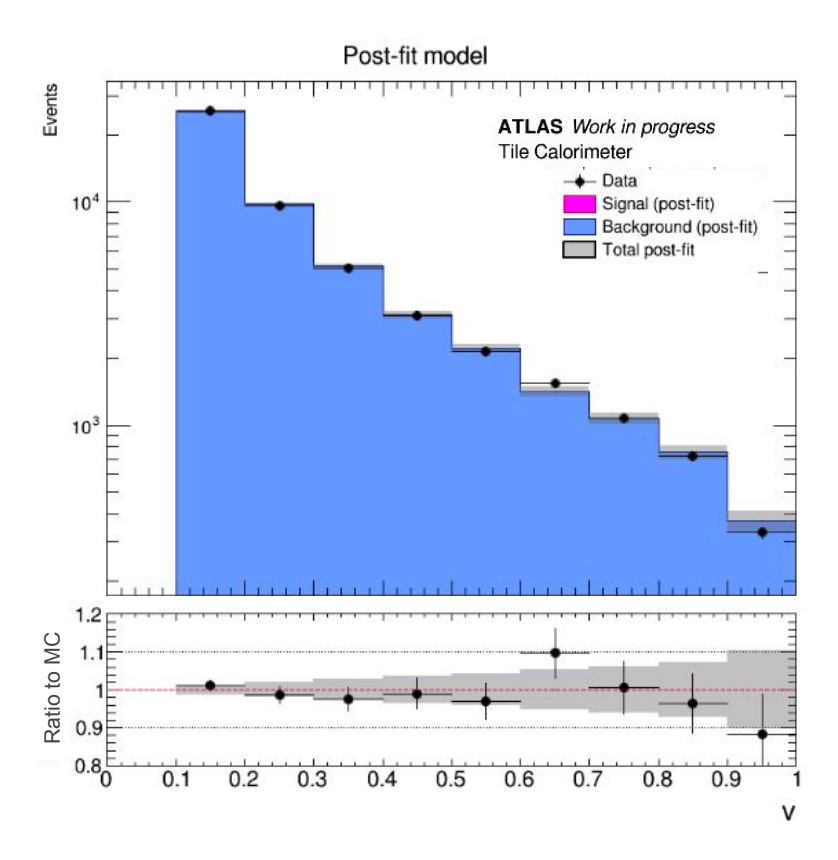
Point estimate

Likelihood-fit: k fixed & k free ($v \ge 0.1$)



- K fixed (K = N_{Data}/N_{MC} = 3.87 ± 0.04)
 - Best-fit μ = 0.74 ± 0.21
- ◆ K profiled (K nuisance parameter)
 - Best-fit μ = -0.12 ± 0.42
 - Best-fit $k = 3.96 \pm 0.04$
- A negative value of μ indicates that the analysis is not sensitive to the signal and that the background dominates.

Post-fit distributions for v > 0.1 (*k free*)



 No significant discrepancies with the data are observed.

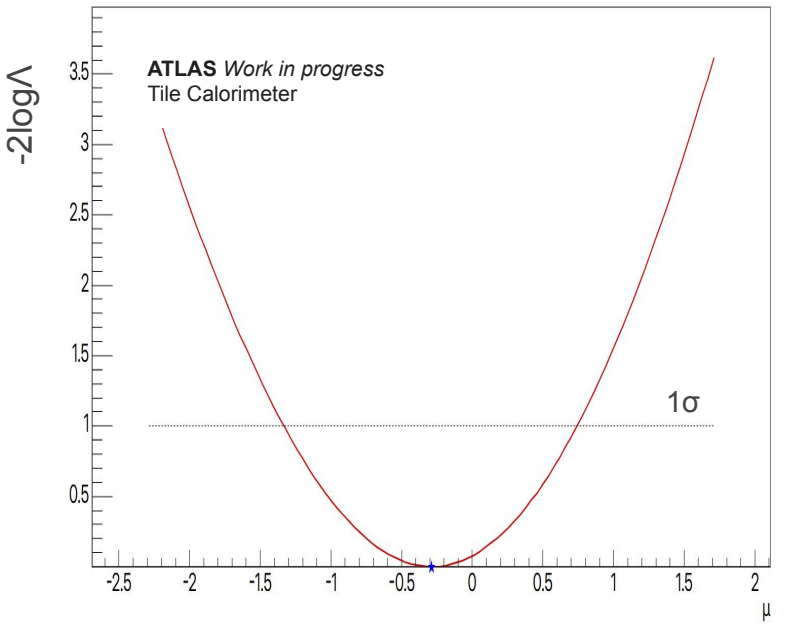
Likelihood-fit with nuisance parameters

- Included 20 parameters in the model:
 - μ, K parameters we are interested in
 - S_i, B_i nuisance parameters to take into account the MC fluctuation of the signal and the background in each bin (18 total nuisance parameters)
- ◆ The negative log-likelihood is, in this case, the sum of 27 terms:

$$-2\log\mathcal{L} = \sum_{i=1}^{N_{ ext{bins}}} \left[2igg(
u_i - n_i \ln
u_i igg) + 2igg(S_i - s_i^{MC} \ln S_i igg) + 2igg(B_i - b_i^{MC} \ln B_i igg)
ight]$$

where
$$\nu_i = k \cdot (\mu \cdot S_i + B_i)$$

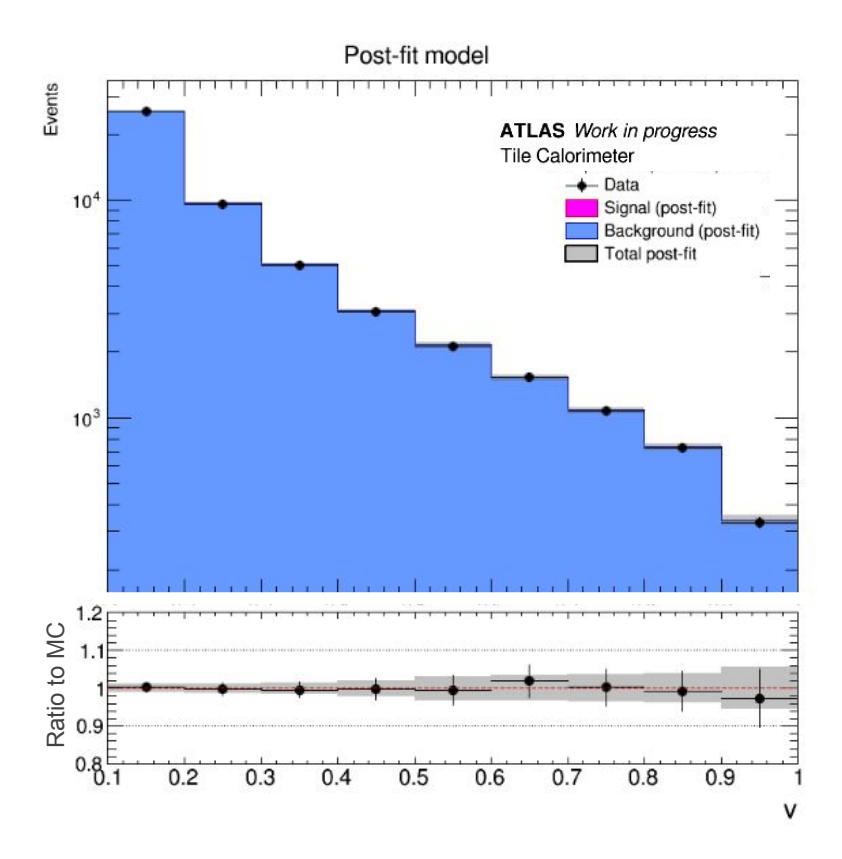
- n_i : observed number of events in bin i
- S_i , B_i : free parameters for signal and background yields in bin i
- $oldsymbol{s}_i^{MC}, b_i^{MC}$: expected values from Monte Carlo templates in bin i
- k: global scaling factor
- μ: fixed signal strength parameter
- $N_{\rm bins}$: total number of bins



Best-fit $\mu = -0.29 \pm 1.07$ Best-fit $k = 3.97 \pm 0.09$

 The uncertainty on μ increases due to contributions from multiple nuisance parameters.

Post-fit distribution for v > 0.1 (with nuisance parameters)



 Taking into account the nuisance parameters for both signal and background improves the agreement between data and the Monte Carlo prediction.

Confidence intervals

Method choice and motivations

- ◆ The standard approach for obtaining precise confidence intervals is the Feldman-Cousins method, which applies Likelihood Ratio (LR) ordering.
- The Feldman–Cousins procedure requires generating pseudo-data to ensure correct frequentist coverage of the intervals. In this analysis, however, Asimov data will be used.
 - **Pseudo-data** are random simulations of the experiment, generated by drawing numbers from probability distributions (typically Poisson) centered around the expected values of the model.
 - The **Asimov dataset** is a deterministic dataset (without statistical fluctuations) that represents the "average" expected experiment under a given hypothesis (in this case, with fixed µ).

Likelihood ratio ordering

- Choose one value for m, m₀ and generate simulated pseudodata accordingly.
- 2. For each observation x calculate (i) the value of the likelihood at mo, p(x|mo)=L(mo) and (ii) the maximum likelihood L(m) over the space of m values.
- 3. Rank all x in decreasing order of likelihood ratio LR=Lx(m0)/Lx(m)
- 4. Accumulate starting from the x with higher LR until the desired CL is reached.
- 5. Repeat for all m

As the likelihood is metric-invariant so is the ratio of likelihoods. Therefore LRordering preserves the metric, mostly avoids empty confidence regions and has several other attractive features. By far the most popular ordering in HEP.

its ordering, and accumulation is done for each given m0.

Take LR-ordering as default option unless there are strong motivations against it.

- By assuming the asymptotic approximation, the distribution of the likelihood ratio statistic asymptotically follows a χ^2 distribution with degrees of freedom equal to the number of parameters being tested.
- In this case, likelihood-based confidence intervals can be used. These intervals are constructed by finding the parameter values for which the likelihood ratio falls within a certain threshold, typically determined by the chi-square distribution under the asymptotic approximation.

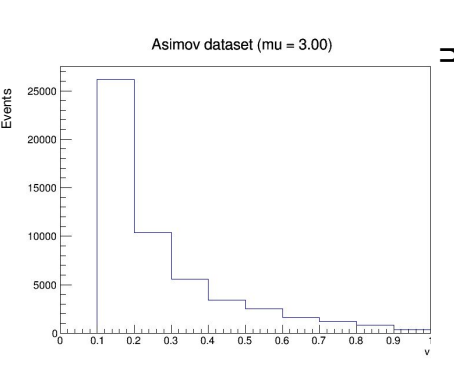
m0 is "true" value

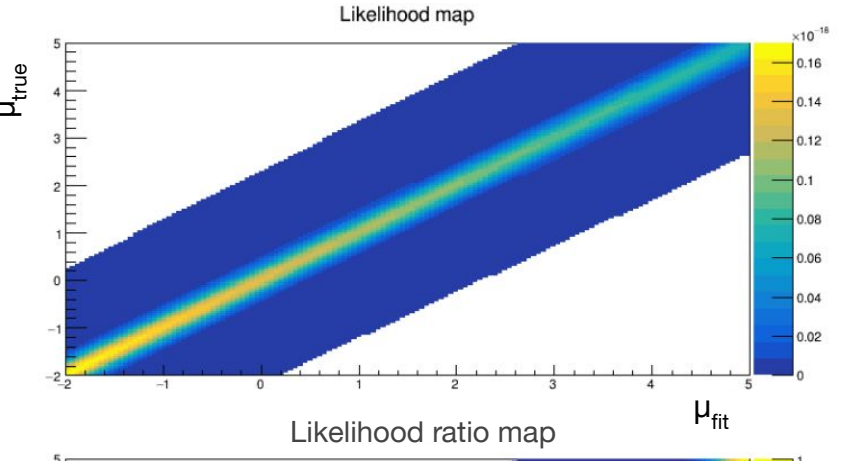
the pseudo data is data generated based on m0

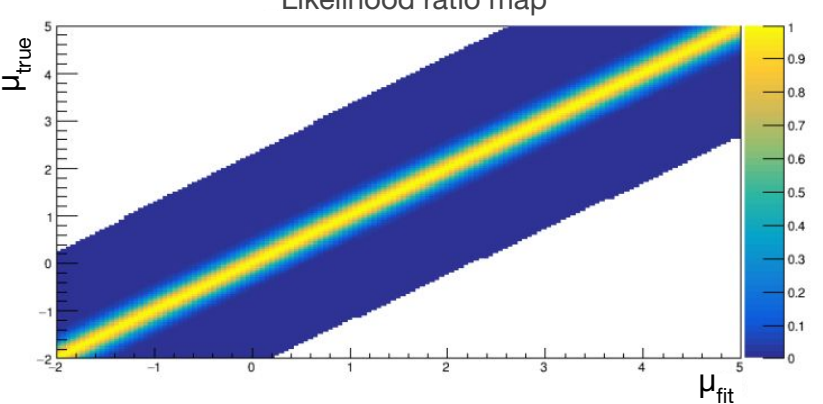
 $LR=L_{m_0}/L_{m_0}$

Asimov data & Likelihood 2D map

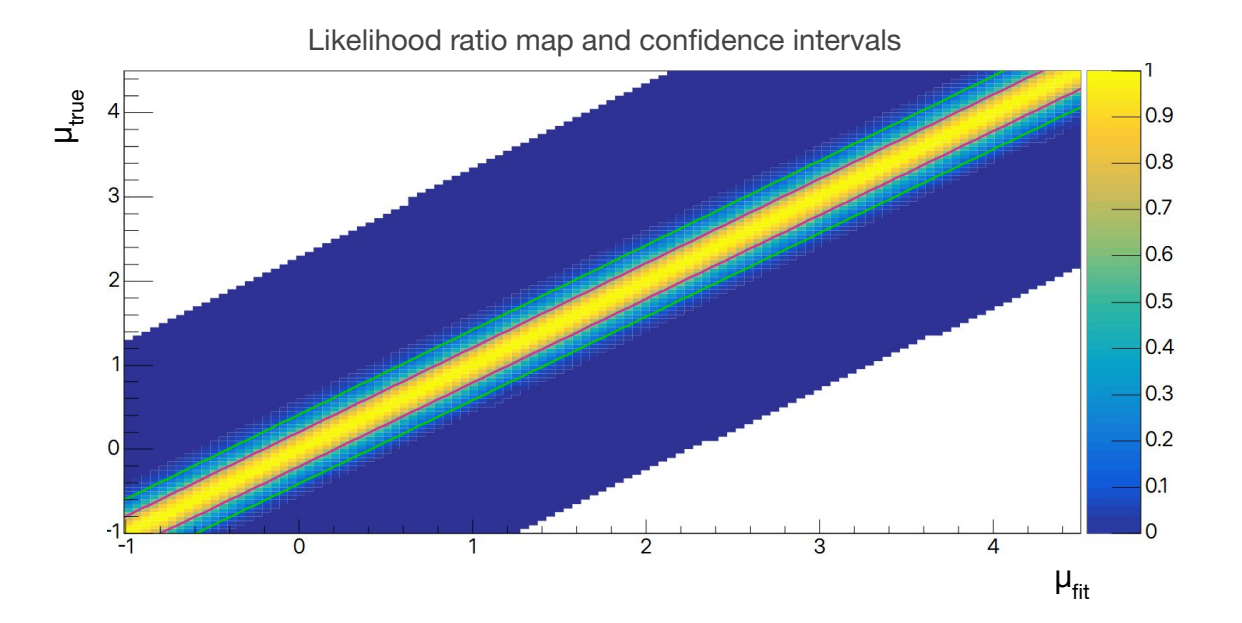
- 140 Asimov datasets were generated with different μ_{fit} between
 -2 and 5 using ν_i= k_{best}*(μ_{fit}*s_i+b_i).
- K_{best} = 3.96 ± 0.04 has been fixed by the likelihood fit with 2 parameters (μ and k, slide 15)
- For each column (corresponding to a given μ_{fit} dataset), the likelihood is plotted as a function of μ_{true} in the range [-2, 5].
- ◆ Each column therefore represents the likelihood profile of the dataset in the y-z plane (**Likelihood map**).
- For each column, the maximum likelihood is found, and all bin contents are normalized to this maximum (Likelihood ratio map).







Confidence intervals (1 σ and 2 σ)



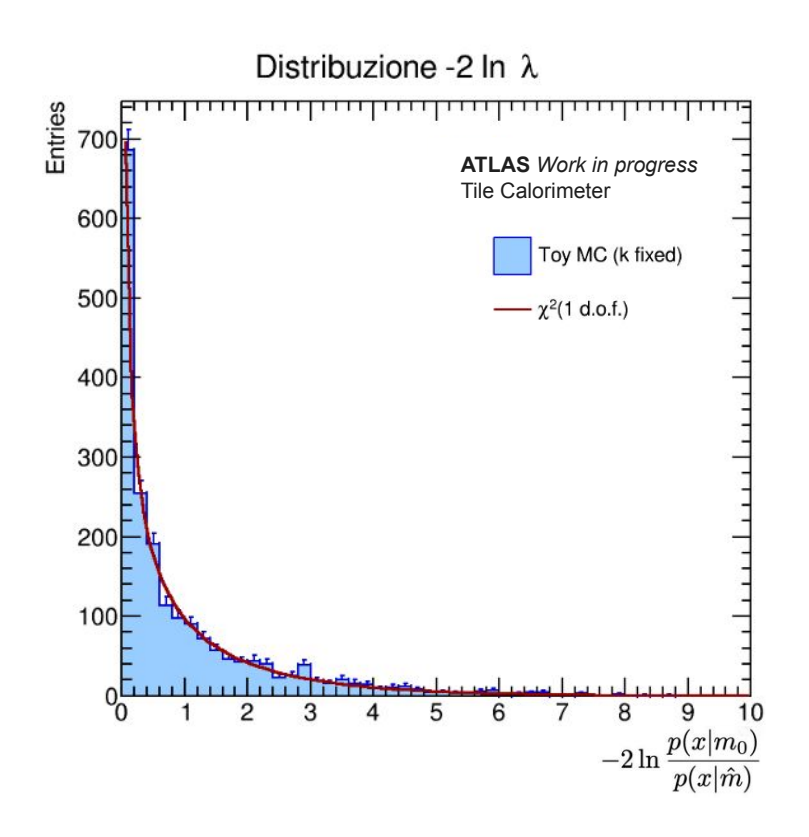
- The 68% (red) and 95% (green) confidence intervals are obtained from the -2logΛ distributions (as a function of μ_{true}), using the threshold:
 - $-2\log\Lambda = 1 (1\sigma)$
 - $-2\log\Lambda = 4 (2\sigma)$

Testing the validity of the Asymptotic Approximation

• Asymptotically (large N), the likelihood ratio distribution approaches the χ^2 distribution.

$$f_k(x)=rac{1}{2^{k/2}\Gamma(k/2)}x^{k/2-1}e^{-x/2}$$
 per $x>0$ $\Gamma(k/2)=\sqrt{\pi}rac{(k-2)!!}{2^{(k-1)/2}}$ per k dispari

- The number of free parameter, in this case, is k=1 (μ).
- The distribution in the plot has been obtained generating 2000 toys with k_{hest} and µ = 2.
- The χ^2 distribution with one degree of freedom is consistent with the likelihood ratio test statistic obtained from the generated toy datasets, confirming the validity of Wilks' theorem.
- This confirms that the asymptotic approximation holds, and likelihood-based confidence intervals can be reliably used.



Conclusions

- This analysis constitutes a <u>very preliminary</u> statistical study of muon photoproduction reactions in iron using data from the TileCal test beam, a study not previously carried out in this form.
- The goal of the analysis is the point estimation of the signal strength and the determination of its confidence intervals.
- ◆ The analysis, affected by a suboptimal choice of observable and a limited number of MC events, is largely insensitive to the signal and dominated by background.
- ♦ However, the analysis is useful for understanding how to improve it and for defining the next steps.

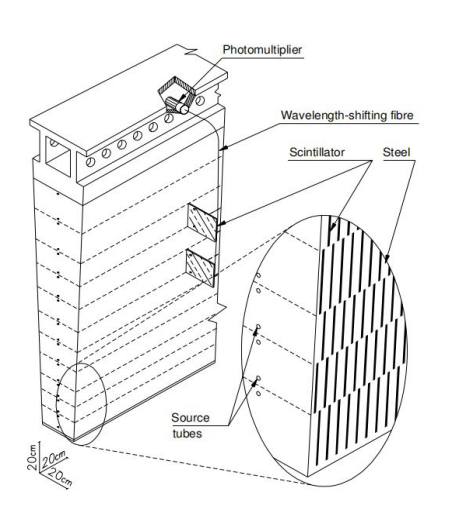
Next steps:

- Increase the number of simulated MC events in the ongoing version of the analysis.
- **Investigate alternative observables** that better separate signal and background, since in the current observable both populate the same bins.
- Use pseudodata to apply likelihood ratio ordering and estimate confidence intervals with the Feldman-Cousins method, also including nuisance parameters.

Backup

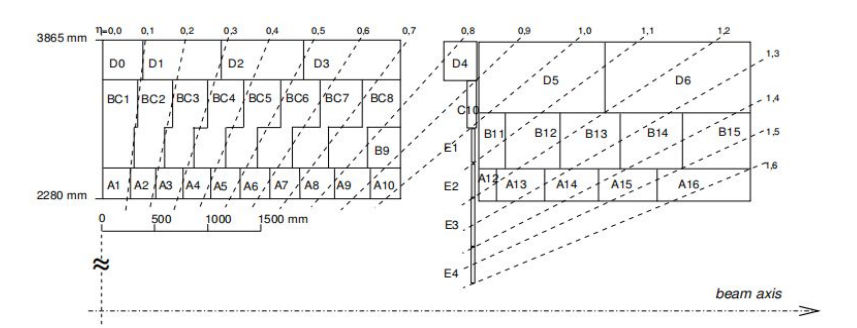
Tile Calorimeter

- ◆TileCal ($|\eta|$ < 1.7) is the central section of the hadronic calorimeter of the ATLAS experiment.
- ◆Sampling calorimeter, composed by scintillating tiles (active material) and steel absorbers.
- ◆The light produced in the scintillating tiles by crossing particles is collected by WaveLength-Shifting fibers (WLSs) and transmitted to PMTs.



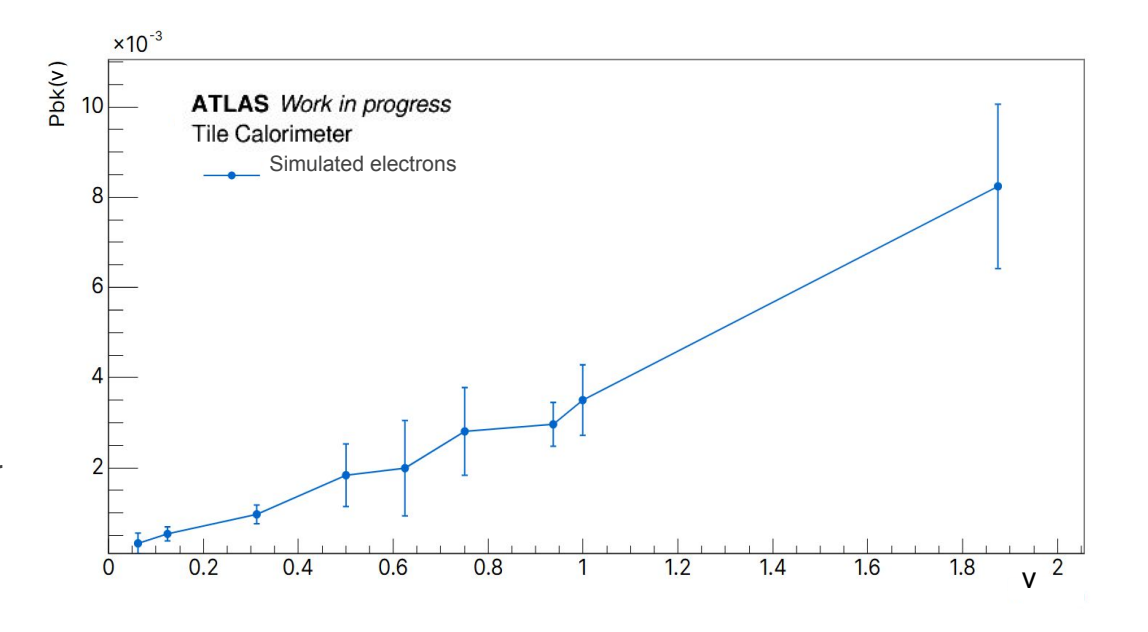


- 4 partitions;
- 64 modules (in each partition), divided in cells read by 2 PMTs.



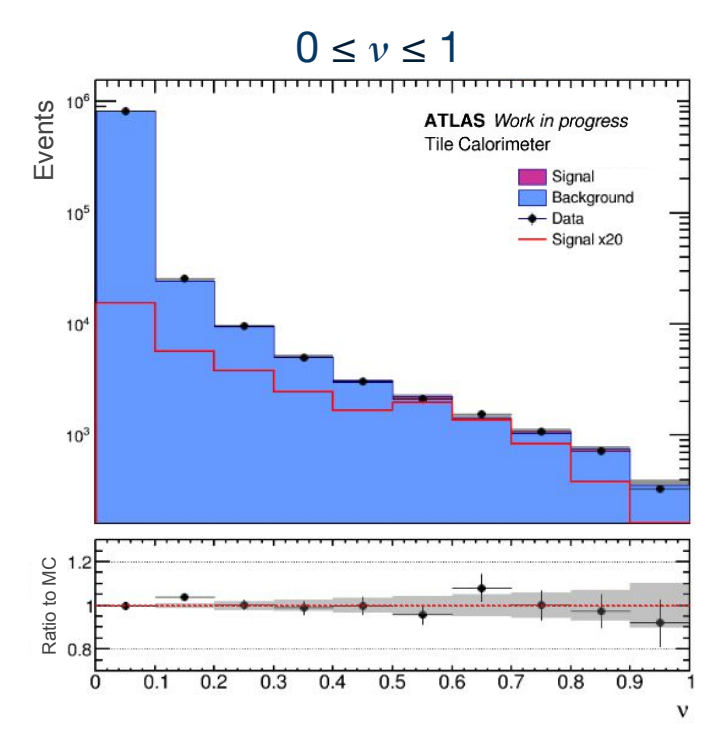
Electron background probability

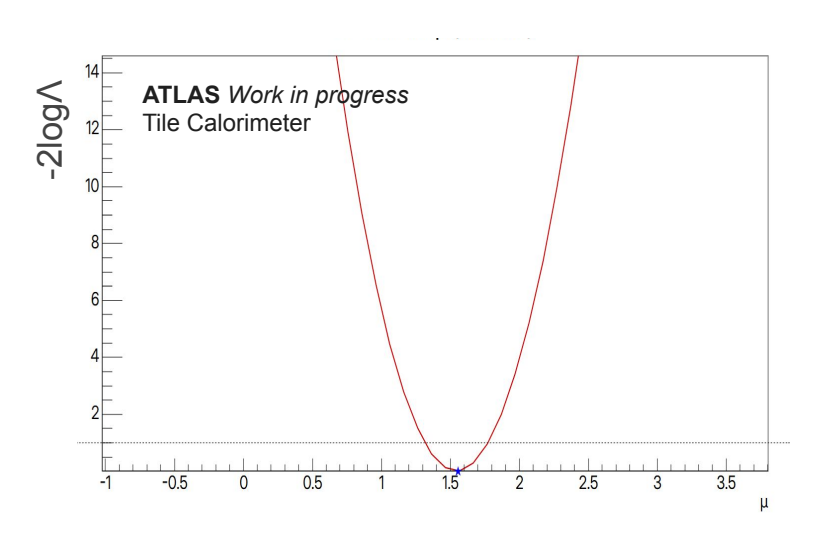
- ◆ Lateral leakage of electromagnetic showers: produced by knock-on electrons or radiative losses of muons (main background source for photonuclear processes)
- ◆ Simulated electron events at +90 (theta) with energies 10, 50, 80, 100, 150 GeV have been used to evaluate the probability that an electron entering at 90 degrees in TileRow 7 produces at least one cell outside the typical muon trajectory with an energy deposit greater than 0.75 GeV.



- For each energy value, six independent simulations were performed, each consisting of 5000 events. The central value corresponds to the mean of the six simulations, while the uncertainty is given by their standard deviation.
- The probability derived from 90-degree electron runs collected at the 2025 test beam will be included in the plot for comparison.

Likelihood-fit: k free $(0 \le v \le 1)$



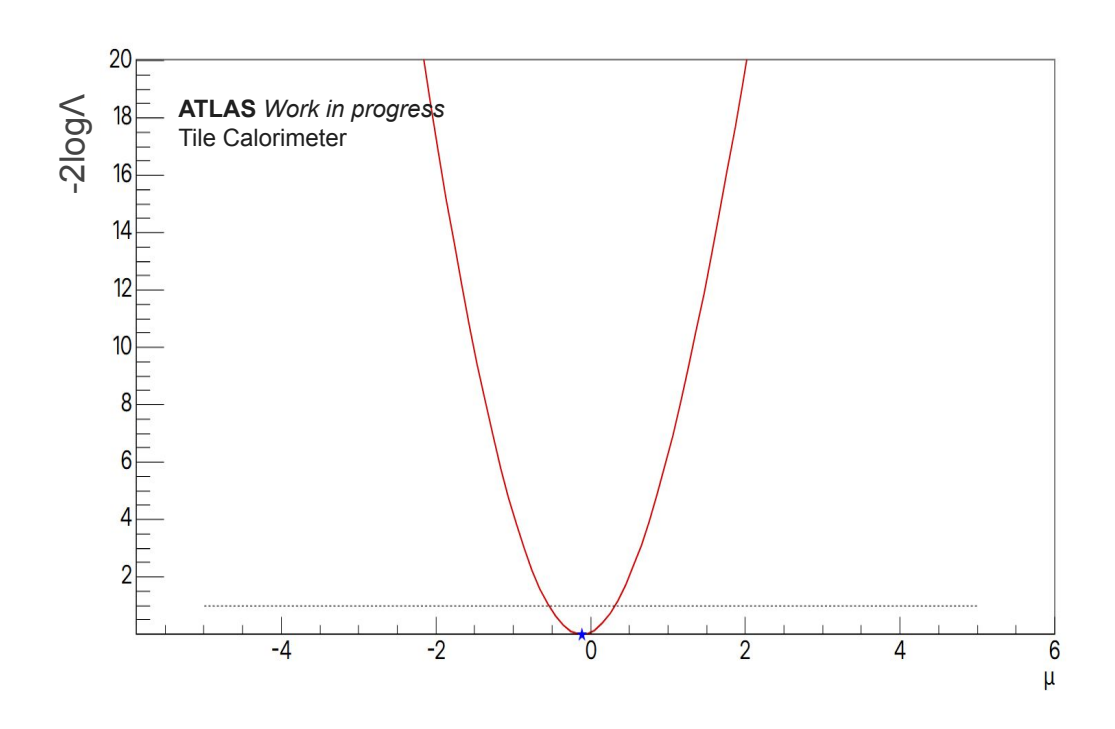


K profiled (K free parameter)

Best-fit μ = 1.56 ± 0.23 Best-fit k = 3.798 ± 0.004

- The central value shifts due to the increased contribution from the background.
- ◆ A method to accurately evaluate the electron background contribution in the first bin is necessary (currently under study in the full analysis).

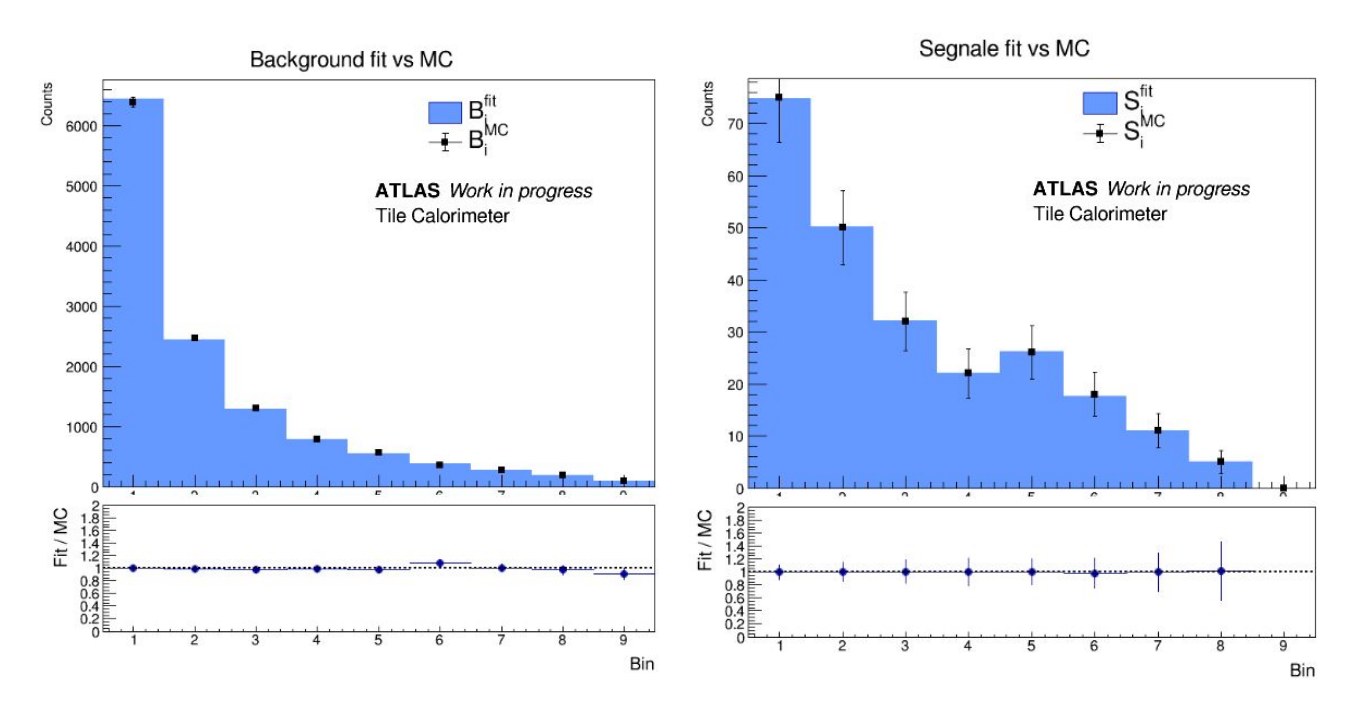
Likelihood-fit with a background scale factor



$$v = k * (\mu * s + a * b)$$

Best-fit μ = -0.11 ± 0.43 Best-fit k = 3.91 ± 0.57 Best-fit a = 1.01 ± 0.15

Nuisance parameter results vs MC (signal & bkg)



• Comparison between the MC signal and background in each bin and the results of S_i and B_i as nuisance parameters.